Drop Formation from Cylindrical Jets in Immiscible Liquid Systems

BERNARD J. MEISTER and GEORGE F. SCHEELE

Cornell University, Ithaca, New York

A theoretical analysis is presented for predicting the size of drops formed from a laminar cylindrical jet when one Newtonian liquid is injected through a nozzle into a second immiscible Newtonian liquid. The analysis couples stability theory with the requirement that the disturbances travel at the same velocity as the jet interface. Comparison of the theory with experimental data for thirteen mutually saturated liquid-liquid systems covering a wide range of physical properties shows a mean error of 11.7% in prediction of the specific surface.

It is generally agreed that the size of drops formed from laminar cylindrical jets is controlled by the amplification of disturbances which result from surface tension instability. Tyler (*15*) was the first investigator to apply Rayleigh's instability theory to the prediction of the drop size. He reasoned that if waves of length, λ, are formed on a cylindrical jet, the volume of the resulting drop should be equal to the volume of a cylinder having the radius, a, of the jet and length λ. The drop volume V_F is then given by

$$V_F = \pi a^2 \lambda \tag{1}$$

where the wave length of a wave is related to the dimensionless wave number ka by the equation

$$\lambda = \frac{2\pi a}{ka} \tag{2}$$

In terms of the dimensionless wave number, Equation (1) becomes

$$V_F = \frac{2\pi^2 a^3}{(ka)_{\max}} \tag{3}$$

where $(ka)_{\max}$ is the wave number of the dominant wave predicted by instability theory. Tyler substituted the nozzle radius a_N for the jet radius and used the *ka* value of 0.696 obtained from Rayleigh's analysis for inviscid liquid jets in air (*10*). He found that the predicted volumes agreed with his experimental data for water jets in air. The data of Merrington and Richardson (*9*) for liquid jets in air also agreed well with the predictions of Equation (*3*). In both of these studies drop size was quite uniform and independent of velocity up to the critical velocity at which jet disruption occurred.

In liquid-liquid systems drop sizes are generally not as uniform as in liquid-air systems. Data are generally reported in terms of the interfacial area formed per unit volume of dispersed phase because this parameter is of interest in extraction systems. The specific surface is defined by

$$S_S = 6/D_{SV} \tag{4}$$

where D_{SV} is the Sauter average diameter calculated from the equation

$$D_{SV} = \frac{\sum_i n_i D_{Fi}^3}{\sum_i n_i D_{Fi}^2} \tag{5}$$

Keith and Hixson (*5*) investigated the formation of drops from jets in liquid-liquid systems. For small nozzle diameters their data indicated that the specific surface displayed a sharp maximum at a particular flow rate. This maximum became less pronounced for larger nozzles. They also studied the distribution of drop sizes in the jetting region and found that the standard deviation of drop size increased gradually with velocity until the jet attained its maximum length, after which the standard deviation increased sharply due to the more random breakup mechanism.

In another experimental study of liquid-liquid systems, Siemes and Kauffman (*14*) showed that the most important parameters controlling drop size were the nozzle diameter, injection velocity, interfacial tension, and the density difference between the phases. They presented empirical correlations in terms of these parameters to predict the maximum specific surface and the velocity at which it occurs.

Christiansen (*1, 2*) derived an equation to predict the drop size at the maximum surface area point in liquid-liquid systems. He modified Tyler's analysis to obtain the equation

$$V_F = \frac{2\pi^2 a_L^3}{(ka)_D} \tag{6}$$

where $(ka)_D$ is the dimensionless wave number predicted by Christiansen's (*1*) instability equation for nonviscous liquid jets in nonviscous liquids, and a_L is the jet radius at the end of the jet. Chistiansen predicted a_L from a graphical correlation of $2a_L/D_N$ vs. the ratio of the interfacial tension to the density difference. He also presented a method of predicting the velocity U_{MS} at which the maximum specific surface occurred. This involved the relation

$$\frac{U_{MS}}{c} = 2.33 \tag{7}$$

where c is the celerity or inherent velocity of the sinuous

Bernard J. Meister is with The Dow Chemical Company, Midland, Michigan.

waves. Christiansen evaluated the celerity from the low velocity instability equation he derived. However, it has been shown (*8*) that if the jet velocity is included in the instability equation derivation, the celerity of the sinuous waves becomes imaginary at the jet velocities in question. Thus, no theoretical significance can be attached to Equation (7).

Shiffler (*13*), in an experimental study of jets in liquid-liquid systems, found that the drop sizes predicted by Equation (6) were generally low. He modified Equation (6) with a snap-off constant, B, to obtain

$$V_F = \frac{2B\pi^2 a_L^3}{(ka)_D} \qquad (8)$$

B was found to be a function of the interfacial tension, decreasing from 6.0 for an interfacial tension of 1.8 dyne/cm. to 1.7 for an interfacial tension of 40 dyne/cm. Shiffler attributed the snap-off constant to inertial and elastic rebound effects at the point of breakoff.

None of the equations in the literature satisfactorily predicted the drop size over the entire range of properties studied in the present investigation. The predictions of Christiansen and Shiffler can be improved for viscous systems by using the value of $(ka)_{max}$ obtained from the general liquid-liquid correlations of Meister and Scheele (*7*) in place of $(ka)_D$ which is valid only for inviscid liquids, but this change alone is not sufficient to produce satisfactory agreement between theory and experiment. This paper presents an improved model for predicting drop size in liquid-liquid systems.

EXPERIMENTAL PROCEDURE

The experimental apparatus is described in a previous paper (*12*). In brief, one liquid was injected into a stationary continuous phase of a second immiscible liquid through a long straight nozzle, and the resulting drop formation was recorded photographically. Still pictures were taken to determine the drop size and drop size distribution, and high speed movies were employed to study the mechanism of drop formation. Fifteen liquid-liquid systems with a wide range in physical properties were studied. Thirteen systems were mutually saturated to eliminate mass transfer effects. To investigate the effects of mass transfer, the benzene-water-acetone system was employed. Runs were made first with 5 wt. % acetone in the dispersed phase (benzene) and then with 5 wt. % acetone in the continuous phase (water). A table of the properties is presented elsewhere (*6, 12*). The specific surface formed for a given system was calculated from Equation (5) by using the average of the major and minor drop diameters as the representative spherical drop diameter.

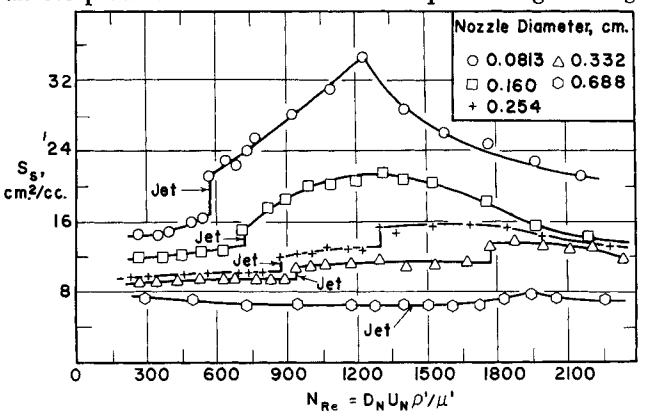

Fig. 1. Effect of injection velocity and nozzle diameter on specific surface for heptane injection into water.

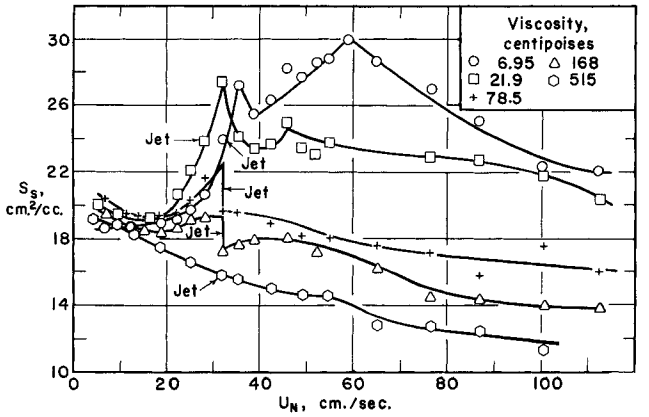

Fig. 2. Effect of injection velocity and continuous phase viscosity on specific surface for heptane injection into aqueous glycerine solutions through 0.0813 cm. diameter nozzle.

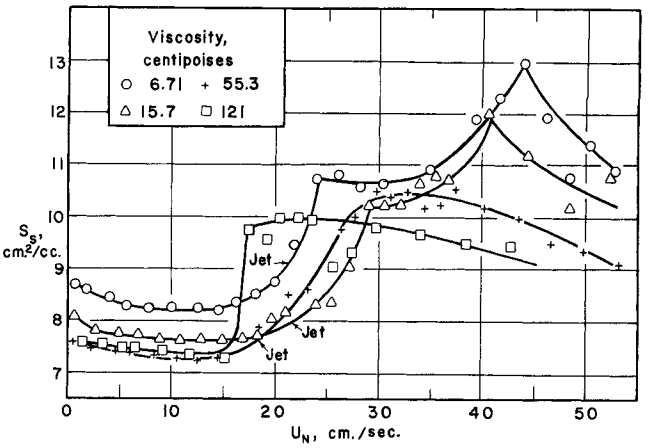

Fig. 3. Effect of injection velocity and dispersed phase viscosity on specific surface for paraffin oil-heptane mixtures injected into water through 0.254 cm. diameter nozzle.

Representative data illustrating the effect of the several variables on the measured specific surface are presented in Figures 1, 2, 3, and 4. Figure 1 shows the specific surface in the heptane-water system as a function of the Reynolds number for five nozzle diameters. Drop size becomes smaller and consequently specific surface higher as the nozzle diameter is decreased. The specific surface shows an abrupt increase at the velocity at which the jet first forms for all but the largest nozzle. This jet formation velocity has been predicted theoretically by Scheele and Meister (*12*). The specific surface then goes through a maximum and decreases at high velocities due to the more random breakup mechanism discussed by Meister and Scheele (*8*). Two of the nozzles in Figure 1 show a step increase in the specific surface at the velocity where the jet increases in length due to the merging of drops (*8*). This effect is mainly a result of the greater jet contraction observed in longer jets.

Figure 2 shows the effect of the continuous phase viscosity on the specific surface for heptane injection into various concentrations of aqueous glycerine solutions through a 0.0813 cm. diameter nozzle. The continuous phase viscosity has only a small effect on the drop size at low velocities prior to jetting, but the effect increases as the velocity increases. This is due to the drag force which increases directly with increasing velocity. Because none of the equations discussed previously consider the continuous phase viscosity, they cannot predict this behavior.

The effect of the dispersed phase viscosity on the specific surface is illustrated in Figure 3 for several heptane-paraffin oil mixtures injected into water through a 0.254 cm. diameter nozzle. The most noticeable effect of an increase in dispersed phase viscosity is a decrease in the specific surface in the jetting region. At very high velocities, this is due to the viscous resistance to atomization of the jet into small drops. At lower velocities where the jet breaks up due to symmetrical capillary waves, the larger drops result from an increase in the dominant wavelength, as predicted by the calculations of Meister and Scheele (*7*).

Figure 4 illustrates the effect of the ratio of the interfacial tension to the density difference $\sigma/g\Delta\rho$ on the specific surface for injection of dispersed phase liquid through a 0.0813 cm.

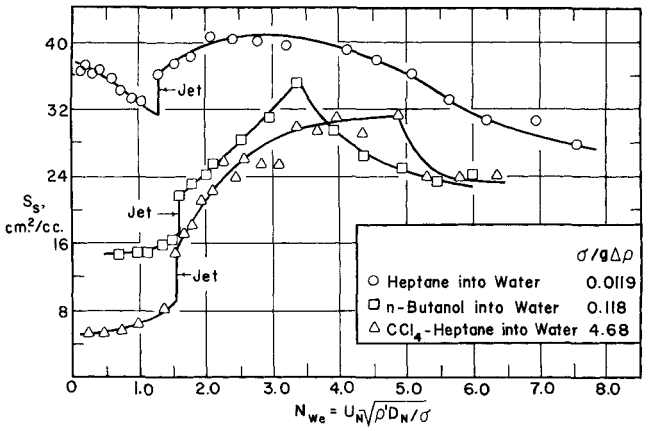

Fig. 4. Effect of Weber number and ratio of interfacial tension to density difference on specific surface for injection through 0.0813 cm. diameter nozzle.

diameter nozzle. Previous articles have shown that the initial jetting velocity (*12*) and the velocity of jet disruption (*8*) are mainly functions of the Weber number, so this function was used as the abscissa in Figure 4 to align the widely differing systems. In the drop formation region prior to jetting, the specific surface shows a strong dependence on the group $\sigma/g\Delta\rho$. As the injection velocity approaches zero, the drop volume is a function only of this parameter for a fixed nozzle diameter. The effect of this group is less pronounced in the jetting region and the curves tend to approach one another as the velocity increases. The effect of $\sigma/g\Delta\rho$ on the specific surface in the jetting region is partly due to jet contraction. For low interfacial tension systems jet contraction is large, whereas for low density difference systems the jet diameter is essentially independent of distance from the nozzle exit.

THEORY

The success of Equation (3) in predicting drop volumes when liquids are injected into gases indicates that stability analysis is a valid starting point for predicting drop formation from jets. The inability of modified forms of this equation to predict satisfactorily drop volumes in liquid-liquid systems suggests that the presence of the liquid continuous phase has not been accounted for adequately. Specifically, none of the previous analyses has considered the effect of the velocity gradient in the jet which arises as a result of the continuous phase viscosity.

Meister and Scheele (*8*) found that the disturbance nodes on the jet surface move at the interfacial velocity of the jet. There must then be a net flow of dispersed phase relative to the disturbance nodes on the jet surface, because the velocity of the interface is less than the average jet velocity. Since the ratio of the interfacial to the average velocity increases with distance from the nozzle exit, the flow relative to the nodes causes a continuous increase in the volume of dispersed phase liquid contained between two given nodes. This behavior is illustrated by jets (A) and (B) in Figure 5. A similar phenomenon is not observed for liquid jets in gases because the velocity profile is essentially flat.

Analyses which use the jet diameter at the point of breakup together with the dimensionless wave number predicted by stability theory are assuming that when the cross-sectional area of the jet changes, the nodes move with respect to the surface to maintain a constant wavelength. Since this assumption is contrary to experimental observations, an alternate hypothesis is necessary.

The volume V_F of a drop formed can be written in general as

$$V_F = Qt_N \tag{9}$$

where Q is the volumetric flow rate of dispersed phase and t_N is the time interval between initiation of successive nodes of the most unstable wave. At steady state all nodes experience the same interfacial velocities as they travel away from the nozzle, so at any instant of time a given node must be able to travel to the position of the preceding node in the time t_N. Therefore, although the distance between nodes increases with distance from the nozzle exit, the time interval between successive nodes remains constant.

If it is assumed that the nodes travel at the jet interfacial velocity U_I, t_N is given by

$$t_N = (\lambda/U_I)_Z \tag{10a}$$

where λ and U_I are the wavelength and interfacial velocity at an axial distance Z halfway between the two nodes. This equation assumes a linear change in λ and U_I between the two nodes. While Equation (10*a*) is valid at all Z, λ can be predicted from stability theory only for small values of Z because the phenomenon of flow through the nodes increases the wavelength above the theoretical value as Z increases. Consequently, to predict t_N theoretically from stability theory, t_N must be evaluated as close to the nozzle as possible, that is at the average position $Z = \lambda/2$ representative of the first wavelength. Equation (10*a*) then becomes

$$t_N = (\lambda_e/U_I)_{\lambda/2} \tag{10b}$$

where λ_e is the most unstable wavelength predicted by stability theory for a jet of radius $(a)_{\lambda/2}$. Substituting Equations (2) and (10*b*) into Equation (9) yields the equation

$$V_F = \frac{2\pi^2(a^3)_{\lambda/2}}{(ka)_{\max}(U_I/U_A)_{\lambda/2}} \tag{11}$$

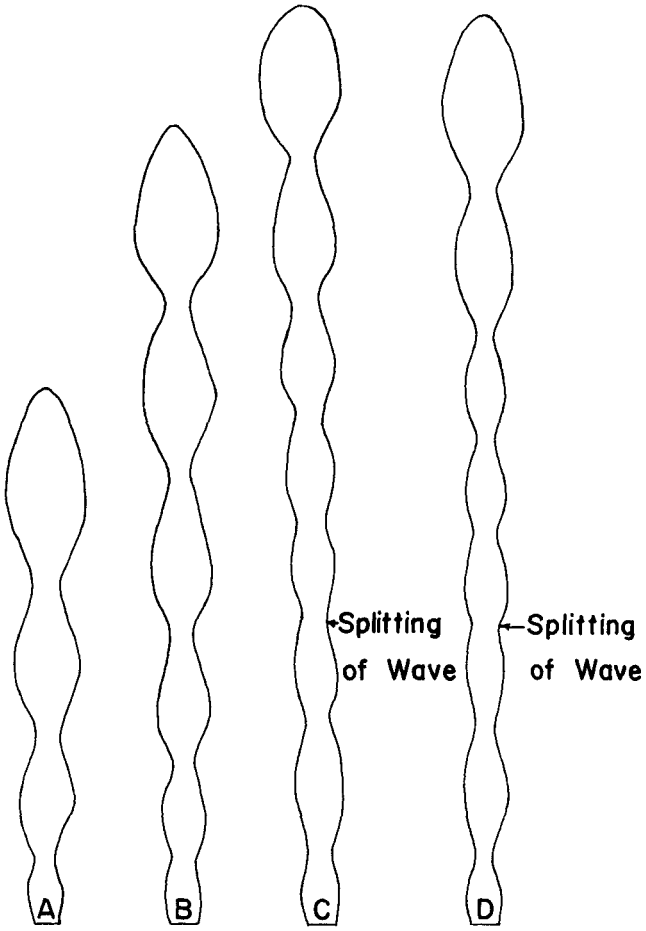

Fig. 5. Illustration of flow through nodes and wave splitting. Tracings from photographs of heptane injection into aqueous glycerine solution through 0.0813 cm. diameter nozzle. A: U_N = 38.5 cm./sec.; B: U_N = 45.4 cm./sec.; C: U_N = 52.0 cm./sec.; D: U_N = 52.0 cm./sec.

Equation (11) would be correct if it were not for the phenomenon illustrated by jets (C) and (D) in Figure 5. Not only does the volume between wave nodes increase due to axial flow through the nodes, but if the volume becomes too large, a new node is formed which splits the original wave in half. Although waves of many lengths have positive growth rates, it is assumed here that only the disturbance which has the theoretical maximum growth rate will split the enlarged wave. Thus, the splitting process will occur only when the distance between nodes becomes greater than two theoretical wavelengths, where the theoretical wavelength is that wavelength predicted by stability analysis. If it is assumed that this new node does not have sufficient time to amplify when the critical wave size is attained during the last wavelength of travel, a critical ratio for splitting can be defined by

$$R_c = \frac{(\lambda)_{L-\lambda}}{(\lambda_e)_{L-\lambda}} \tag{12}$$

where $(\lambda)_{L-\lambda}$ is the actual wavelength at $Z = L - \lambda$ and $(\lambda_e)_{L-\lambda}$ is the wavelength predicted by stability analysis for a jet of radius $(a)_{L-\lambda}$.

Since t_N does not change with distance from the nozzle, Equation (10*a*) can be used to obtain

$$(\lambda)_{L-\lambda} = (\lambda_e)_{\lambda/2} \frac{(U_I)_{L-\lambda}}{(U_I)_{\lambda/2}} \tag{13}$$

and Equation (12) then becomes

$$R_c = \frac{(\lambda_e)_{\lambda/2}(U_I)_{L-\lambda}}{(\lambda_e)_{L-\lambda}(U_I)_{\lambda/2}} \tag{14}$$

Equation (2) can be substituted for λ_e in Equation (14). Since ka is independent of a, Equation (14) becomes

$$R_c = \frac{(U_I)_{L-\lambda}(a)_{\lambda/2}}{(U_I)_{\lambda/2}(a)_{L-\lambda}} \tag{15}$$

If the ratio of interface to average velocity is used, Equation (15) becomes

$$R_c = \frac{(U_I/U_A)_{L-\lambda}(a^3)_{\lambda/2}}{(U_I/U_A)_{\lambda/2}(a^3)_{L-\lambda}} \tag{16}$$

The equation for drop volume resulting from jet instability can then be expressed generally as

$$V_F = \frac{2\pi^2(a^3)_{\lambda/2}}{N(ka)_{\max}(U_I/U_A)_{\lambda/2}} \tag{17}$$

where N is a function of R_c. If R_c is less than two, the wave does not split and N equals one; if R_c is greater than two but less than four the wave splits once and N equals two; if R_c is greater than four but less than eight the wave splits twice and N equals four, etc. The largest value of N observed over the wide range of experimental variables investigated in this study was four.

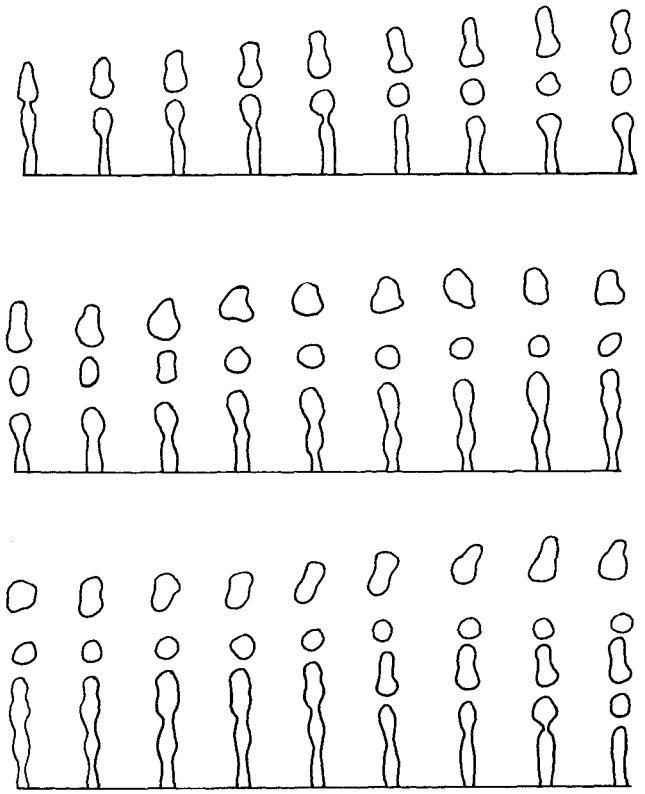

Fig. 6. Illustration of alternation between force balance and instability mechanisms of drop formation. Tracings from 2,500 frames/sec. movie for heptane injection into water through 0.254 cm. diameter nozzle at nozzle velocity = 22.0 cm./sec. Time interval between successive events is 0.00416 sec.

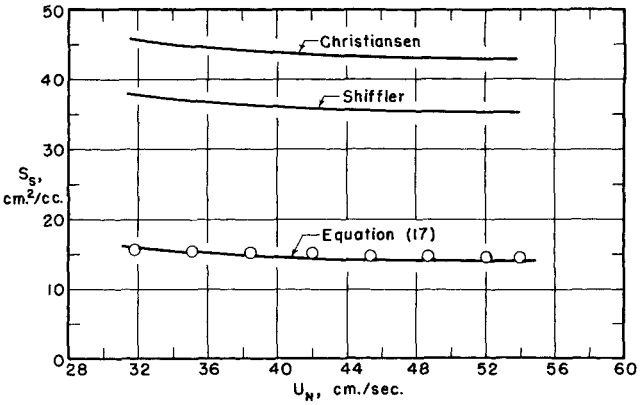

Fig. 7. Prediction of specific surface in jetting region as a function of nozzle velocity for heptane injection into glycerine through 0.0813 cm. diameter nozzle. System has a large continuous phase viscosity: $\mu = 515$ centipoises.

Equation (17) is not valid when the jet length is small because the instability mechanism determines drop size only when the jet length is greater than one wavelength. For these short jets, drop formation is similar to that occurring at the nozzle before a jet forms and is controlled by a force balance on the forming drop. The diameter on which the force balance is based must be the jet diameter at the point of drop necking rather than the nozzle diameter, because the drop is formed from a jet which has undergone some contraction after exit from the nozzle. With this modification, the equation presented by Scheele and Meister (*12*) becomes

$$V_F = F\left[\frac{2\pi\sigma a}{g\Delta\rho} - \frac{4\rho' Q U_N}{3\left(\frac{a}{a_N}\right)^2 g\Delta\rho} + \frac{40\mu Q a}{D_F^2 g\Delta\rho} + 7.15\left(\frac{Q^2 a^2 \rho'\sigma}{(g\Delta\rho)^2}\right)^{1/3}\right] \tag{18}$$

where a, the jet radius one drop diameter from the end of the jet, can be predicted from Shiffler's jet contraction equation (*8, 13*). The calculation is iterative but a reasonable estimate of D_F is generally sufficient to calculate a. The constant 4/3 in the kinetic force term in Equation (18) was obtained by assuming a parabolic velocity profile, which is not exactly true because some relaxation of the profile will take place.

When the jet length is between one and two wavelengths, a regular alternating pattern of drop sizes will occur. After a drop breaks off as a result of the instability mechanism, the remaining jet is less than one wavelength long, and the next drop begins to form by the force balance mechanism. The drops formed in this way are

much larger than the drops which arise from jet instability. The jet length increases sufficiently during the time of formation of these drops that, after the breakoff of a drop formed by the force balance mechanism, the jet is again long enough to be subject to capillary instability. This phenomenon is illustrated in the series of pictures in Figure 6 traced from a 2,500 frames/sec. movie for heptane injection into water through a 0.254 cm. diameter nozzle.

In summary, the equation used to predict drop size is dependent on the jet length. If the jet is less than one wavelength long, Equation (18) should be used; if the jet is greater than two wavelengths long, Equation (17) should be used; and if the jet is between one and two wavelengths long, the mechanisms will alternate to produce an equal number of each size drop.

COMPARISON OF THEORY AND EXPERIMENT

Drop volumes in the velocity region between the initial jetting velocity and the velocity of jet disruption were calculated using Equation (17) or (18), whichever was applicable, and were converted to specific surface by means of Equation (4). These values and the predictions of Christiansen's analysis, Equation (6), and Shiffler's analysis, Equation (8), were compared to the experimental specific surface calculated using the experimental Sauter diameter defined by Equation (5). The experimental jet length and Shiffler's equation for jet contraction were employed in all three predictions. The values of $(ka)_{max}$ obtained from the correlation of Meister and Scheele (7) were used in Equation (17), whereas the values of $(ka)_D$ obtained from Christiansen's equation were used in Equations (6) and (8). The interfacial velocities required in Equation (17) were calculated from the velocity profile equations of Meister and Scheele (8), employing constants appropriate to the particular system.

A table listing the experimental and predicted specific surfaces for the thirteen saturated liquid-liquid systems is presented by Meister (6). The mean error of Equations (17) and (18) over the entire jetting region was 11.7%, whereas the Christiansen and Shiffler predictions had mean errors of 72.9 and 46.3%, respectively. The corresponding maximum errors were 47, 246, and 183%. At the velocity at which maximum specific surface occurs, where Christiansen intended his equation to be applied, the mean errors were 7.8, 68.7, and 42.7%, respectively. Figures 7 to 10 illustrate the predictions of the three methods for four representative systems.

When the experimental jet length is not known, the length can be predicted by using the equations of Meister and Scheele (8). These equations require an estimate of the initial disturbance level. This jet length can be used to determine whether Equation (17) or (18) is applicable and to determine the jet diameters and interfacial velocities required in Equation (16) to evaluate R_C. The resulting error using this procedure is greater because of the additional error associated with the prediction of jet length. Fortunately, the interfacial velocity and jet diameter are fairly insensitive to small changes in jet length so that reasonable predictions of drop size can be made without knowing the jet length precisely.

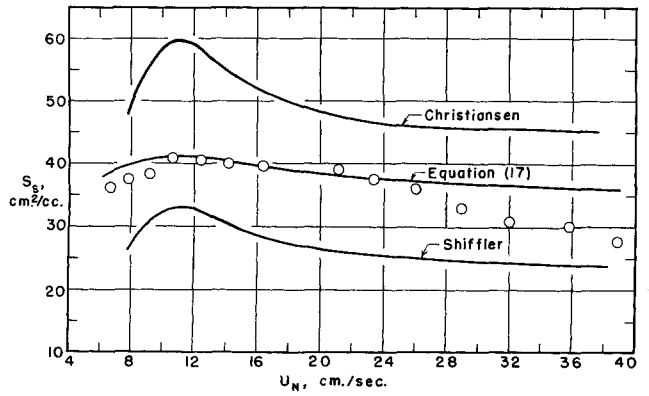

Fig. 8. Prediction of specific surface in jetting region as a function of nozzle velocity for butyl alcohol injection into water through 0.0813 cm. diameter nozzle. System has a low interfacial tension: $\sigma = 1.8$ dynes/cm.

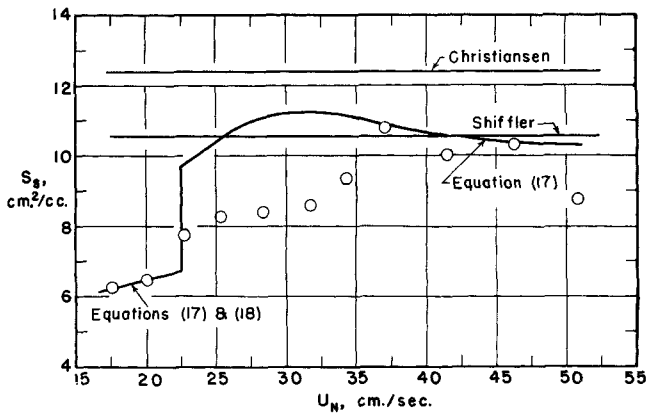

Fig. 9. Prediction of specific surface in jetting region as a function of nozzle velocity for injection of heptane-carbon tetrachloride mixture into water through 0.254 cm. diameter nozzle. System has a low density difference: $\Delta\rho = 0.010$ g/cc.

DISCUSSION OF RESULTS

The present analysis shows better agreement with experimental results than previous analyses, as illustrated in Figures 7 to 10. The most significant improvements in predictions of drop volume which resulted from use of Equation (17) occurred for systems with a high continuous phase viscosity, as shown in Figure 7, and for all systems at low injection velocities where the jet length was short, as shown by the low velocity portions of Figures 9 and 10. For highly viscous continuous phase systems the ratio of the interfacial velocity to the average jet velocity is very low. A comparison of Equations (6), (8), and (17) shows the increasing importance of the parameter U_I/U_A as it deviates from unity, and the good agreement between theory and experiment supports its inclusion in Equation (17). At low injection velocities, the success of the present analysis results from consideration of the alternate mechanisms which control drop size when the jet length is less than two wavelengths, a factor neglected in previous theories.

For every liquid-liquid system and nozzle diameter and at all velocities in the jetting region prior to jet disruption, the present analysis gave better agreement with experimental data than Christiansen's equation. Shiffler's empirical modification was somewhat better than Christiansen's equation because of the use of the snap-off constant B. This constant, which Shiffler attributed to inertial and elastic rebound effects at the point of breakoff, actually helps correct for the use of a_L in Equation (8), since the largest corrections apply to those systems with low interfacial tension where jet contraction is large. It should be pointed out that Shiffler's correlation was established from data for injection through orifice plates under conditions where the velocity profile was essentially flat at the orifice exit, and thus it would not be expected to work as well for the present data where the velocity profile at the nozzle exit was parabolic. Conversely, the present analysis would have to be modified for application to Shiffler's data. The modification of the present theory for new situations requires only the development of expressions for

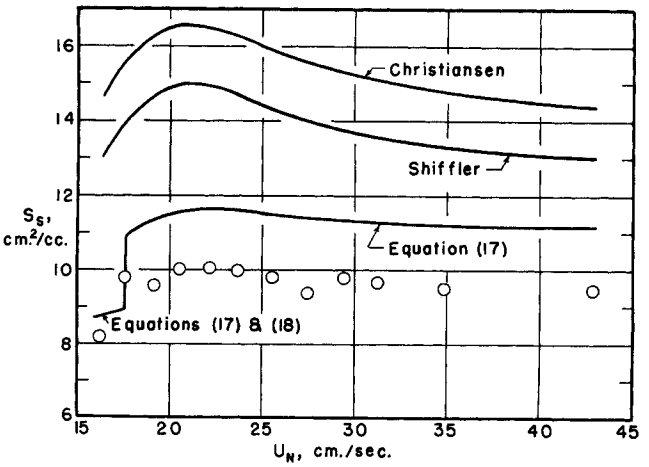

Fig. 10. Prediction of specific surface in jetting region as a function of nozzle velocity for paraffin oil injection into water through 0.254 cm. diameter nozzle. System has a large dispersed phase viscosity: $\mu' = 121$ centipoises.

U_I/U_A, while it is not clear how an empirical correlation can be extended.

In situations where Equation (17) had greater than 10% error, the surface area predictions were generally high and the drop volume predictions correspondingly low. Analysis of the raw data indicated that these systems were invariably the ones where significant drop size distribution occurred. The only drop size distribution mechanism considered in the analysis is that responsible for the alternating pattern observed for short jet lengths and shown in Figure 6. However, several other causes of drop size distribution were observed experimentally.

One of these is a phenomenon similar to the merging of drops which causes the sudden lengthening of a jet described in an earlier paper (*8*). In this situation a drop which has broken off does not have sufficient rise velocity to escape before the jet overtakes it. The drop remerges with the jet, as illustrated in Figure 11, and a drop with twice the original volume ultimately breaks off the jet. This double drop is not recaptured by the jet because it has a higher rise velocity than the single drop. Because of slight fluctuations at the end of the jet, the single drop sometimes escapes and sometimes doesn't. This causes a distribution of drop sizes. In some cases, only double drops are formed. Christiansen referred to this phenomenon as *twinning*. This mechanism occurs in the range of velocities where jet lengthening also occurs, and it is particularly prevalent for small diameter nozzles where the drops decelerate markedly after breaking away because the difference between the jet velocity and the steady state rise velocity is great. A study of the unsteady state rise velocity of drops is necessary before predictions of this phenomenon can be made.

A second mechanism which causes a distribution of drop sizes was observed when paraffin oil was injected into water. Occasionally the second node from the end of the jet broke off rather than the last one, causing the drop to be twice the predicted size. This phenomenon, which is probably due to the cohesiveness of these very viscous jets, causes the discrepancy between theory and experiment shown in Figure 10.

One further cause of drop size distribution is coalescence of drops resulting from collisions after they leave the jet. Because this study was concerned only with jet mechanics, the drops measured were the ones closest to the jet. However, in some systems coalescence occurred so soon after drop breakoff that the experimental distribution measured was not the same as the distribution formed from the jet. Coalescence was particularly significant in systems with low interfacial tensions or low density differences and systems where mass was being transferred out of the dispersed phase. The amount of coalescence increased with nozzle throughput because of the greater number of drops formed at high flow rates. This effect is illustrated by the high velocity data in Figure 8. All of the above-mentioned causes of drop-size distribution will produce larger size drops than those predicted by Equation (17), so specific surface predictions will be high when these mechanisms occur.

In some instances very small satellite drops were formed in addition to the primary drops. Such drops contributed negligibly to the specific surface because the Sauter diameter is weighted towards the large drops. The satellite drops appear to be formed from the neck of fluid drawn out during drop breakoff, as explained by Goren (*3*), and are formed reproducibly at distinct velocities for each system in no apparent logical pattern. An analysis predicting when they will appear seems unlikely, because the magnitude of forces involved in their formation is so small compared to the forces affecting the formation of primary drops.

The large number of drop size distribution mechanisms makes a complete theoretical analysis extremely difficult because many alternatives must be considered. Fortunately, for most cases the complicating factors do not alter the specific surface greatly.

Another improvement which could be made in the theoretical model is the development of a more sophisticated criterion for wave splitting, based on the growth rates of the disturbances. In the present model it has been assumed that when the wavelength actually present on the jet becomes greater than twice the wavelength predicted by stability theory, a new node will form which has a growth rate equal to that predicted by stability theory. A better assumption would be that the wave will split in half when the growth rate of the split wave becomes equal to that of the undivided wave. As a wave on the jet increases in length, its growth rate decreases. Consequently, the wave will split when its length is less than twice that of the most unstable wave, and the split wave will have neither the wavelength nor the growth rate characteristic of the most unstable disturbance. The resulting criterion for wave splitting will be more complex than that presented in this paper.

To predict drop size after wave splitting, it is necessary to determine whether or not a newly formed node will have a sufficiently large amplitude to cause drop breakoff when it reaches the end of the jet. This is difficult because photographs showed that the growth rate of a newly formed node was greater than stability theory predicts, indicating that an interaction effect exists between adjacent nodes, as noted by Rumscheidt and Mason (*11*). It appears that the old nodes have an amplification effect on the newly formed nodes, while the newly formed nodes damp the original ones. This interaction may explain why the predicted jet lengths were shorter than the actual lengths observed for heptane injection into glycerine, a system where much flow through the nodes and sub-

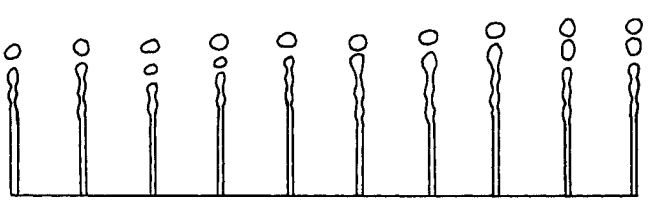

Fig. 11. Illustration of drop size distribution mechanism which is result of drop merging with jet. Tracings from 2,500 frames/sec. movie for heptane injection into water through 0.0813 cm. diameter nozzle at nozzle velocity of 54.0 cm./sec. Time interval between successive events is 0.00166 sec.

sequent wave splitting occurred.

The effect of mass transfer on the size of drops formed from the jet was quite small. The maxima in the specific surface curves for the system with mass transfer into the jet and the pure benzene-water system were about the same. The system with mass transfer out of the jet exhibited a much lower maximum due to the excessive amount of coalescence which took place in this system after drop formation. Groothius and Zuiderweg (*4*) found that mass transfer promotes coalescence when the solute is transferred out of the dispersed phase.

The initial disturbance amplitude, which was changed by placing 200-mesh stainless steel screens in the nozzle at various distances from the exit, had a slight effect on drop size prior to jet disruption. As the disturbance level increased, the drop size distribution became broader. The specific surface also decreased, primarily because the jet length was much shorter and jet contraction consequently smaller. This affects the value of N in Equation (17). An increase in disturbance level may also produce a flatter velocity profile at the nozzle exit, leading to a smaller value of R_C and perhaps a smaller N. If initial disturbances of a particular wavelength and large amplitude were impressed on the system, significant changes in specific surface could result, but such experiments were not conducted in the present study.

Both mass transfer and large disturbances do decrease the velocity of jet disruption (*8*) and therefore lower the velocity limit above which the drop size distribution is excessively broad. This factor must be considered when applying the predictions to practical problems.

SUMMARY

Stability theory can be used to obtain Equation (17) for predicting the size of drops formed from jets when one liquid is injected into a second immiscible liquid at velocities lower than the jet disruption velocity. The generalized solution to the Tomotika stability analysis given by Meister and Scheele (*7*) can be used to predict the dimensionless wave number of the most unstable disturbance. The analysis is complicated by the fact that the disturbances travel at the interfacial jet velocity, so the velocity distribution in the jet must be known. If the dispersed phase velocity profile is initially parabolic, the approximate distribution presented by Meister and Scheele (*8*) can be used. For injection of nonviscous liquids into gases the drop size prediction is considerably simplified because the Rayleigh approximation can be used to predict the dimensionless wave number and because the velocity distribution quickly becomes uniform. The resulting equation is then identical with that originally presented by Tyler (*15*).

Equations for the prediction of jet length have been presented previously (*8*). If the jet has a length less than twice the wavelength of the most unstable wave, drop formation is not always controlled by the instability mechanism but at times by a force balance mechanism similar to that which controls the formation of drops at velocities below that of initial jet formation. Equation (18) predicts the drop volume when the force balance mechanism occurs. If the jet is long and the interfacial velocity is low, splitting of the waves on the surface will occur. An approximate criterion for wave splitting is presented in terms of the parameter R_c defined by Equation (16).

The present analysis gives better agreement with experimental data than previous theories. The low mean error of 11.7% in specific surface predictions for thirteen mutually saturated liquid-liquid systems with a wide range of physical properties lends experimental support to the analysis.

ACKNOWLEDGMENT

The authors gratefully acknowledge the Ford Foundation Fellowship awarded to B. J. Meister.

NOTATION

a = jet radius, cm.
a_L = jet radius at end of jet, cm.
a_N = nozzle radius, cm.
B = snap-off constant in Equation (8)
c = celerity of sinuous wave, cm./sec.
D_F = drop diameter, cm.
D_{SV} = Sauter average drop diameter, cm.
D_N = nozzle diameter, cm.
F = Harkins-Brown correction factor
g = acceleration of gravity, 980 cm./sq. sec.
k = wave number, cm.$^{-1}$
$(ka)_D$ = dimensionless wave number from instability theory for inviscid liquid-liquid systems
$(ka)_{\max}$ = dimensionless wave number of dominant symmetrical wave
L = jet length, cm.
n_i = number of drops of diameter D_{Fi}
N = factor in Equation (17) to account for wave splitting
Q = volumetric flow rate of dispersed phase, cc./sec.
R_c = critical ratio defined by Equation (12)
S_S = specific surface, sq. cm./cc.
t_N = time between initiation of nodes, sec.
U_A = average jet velocity, cm./sec.
U_I = interfacial velocity, cm./sec.
U_{MS} = velocity at which maximum specific surface occurs, cm./sec.
U_N = average dispersed phase velocity at nozzle exit, cm./sec.
V_F = volume of drop, cc.
Z = axial distance from nozzle, cm.

Greek Letters

λ = actual wavelength of dominant wave, cm.
λ_e = wavelength of dominant wave predicted by stability theory, cm.
μ, μ' = viscosities of continuous and dispersed phases, respectively, gm./(cm.)(sec.)
ρ' = dispersed phase density, gm./cc.
σ = interfacial tension, dyne/cm.

LITERATURE CITED

1. Christiansen, R. M., Ph.D. thesis, Univer. Pennsylvania, Philadelphia (1955).
2. ———, and A. N. Hixson, *Ind. Eng. Chem.*, **49**, 1017 (1957).
3. Goren, S., *J. Colloid Sci.*, **19**, 81 (1964).
4. Groothius, H., and F. J. Zuiderweg, *Chem. Eng. Sci.*, **12**, 288 (1960).
5. Keith, F. W., and A. N. Hixson, *Ind. Eng. Chem.*, **47**, 258 (1955).
6. Meister, B. J., Ph.D. thesis, Cornell Univer., Ithaca, N. Y. (1966).
7. ———, and G. F. Scheele, *AIChE J.*, **13**, 682 (1967).
8. *Ibid.*, **15** (1969).
9. Merrington, A. C., and E. G. Richardson, *Proc. Phys. Soc.*, **59**, 1 (1947).
10. Rayleigh, Lord, *Proc. Royal Soc.*, **29**, 71 (1879).
11. Rumscheidt, F. D., and S. G. Mason, *J. Colloid Sci.*, **17**, 260 (1962).
12. Scheele, G. F., and B. J. Meister, *AIChE J.*, **14**, 9 (1968).
13. Shiffler, D. A., Ph.D. thesis, Cornell Univer., Ithaca, N. Y. (1965).
14. Siemes, W., and J. F. Kauffman, *Chem. Ingr. Tech.*, **29**, 32 (1957).
15. Tyler, E., *Phil. Magazine*, **16**, 504 (1933).

Manuscript received August 2, 1967; revision received May 13, 1968; paper accepted May 20, 1968.